


OMA1 competitively binds to HSPA9 to promote mitophagy and activate the cGAS–STING pathway to mediate GBM immune escape

Wen de Zhu,¹ Jin Rao,¹ Li hua Zhang,¹ Ka ming Xue,² Lin Li,¹ Jun jun Li,¹ Qian zhi Chen,³ Rong Fu ¹

To cite: Zhu W, Rao J, Zhang Lhua, *et al.* OMA1 competitively binds to HSPA9 to promote mitophagy and activate the cGAS–STING pathway to mediate GBM immune escape. *Journal for ImmunoTherapy of Cancer* 2024;**12**:e008718. doi:10.1136/jitc-2023-008718

► Additional supplemental material is published online only. To view, please visit the journal online (<https://doi.org/10.1136/jitc-2023-008718>).

WdZ and JR contributed equally. QzC and RF contributed equally.

Accepted 03 April 2024



© Author(s) (or their employer(s)) 2024. Re-use permitted under CC BY-NC. No commercial re-use. See rights and permissions. Published by BMJ.

¹Department of Neurosurgery, Union Hospital, Tongji Medical College, Huazhong University of Science and Technology, Wuhan, Hubei, China

²Department of Traditional Chinese Medicine, Union Hospital, Tongji Medical College, Huazhong University of Science and Technology, Wuhan, Hubei, China

³Department of Breast and Thyroid Surgery, Huazhong University of Science and Technology, Wuhan, Hubei, China

Correspondence to
Professor Rong Fu;
furonglp@163.com

ABSTRACT

Background Immunotherapy with checkpoint inhibitors, especially those targeting programmed death receptor 1 (PD-1)/PD-1 ligand (PD-L1), is increasingly recognized as a highly promising therapeutic modality for malignancies. Nevertheless, the efficiency of immune checkpoint blockade therapy in treating glioblastoma (GBM) is constrained. Hence, it is imperative to expand our comprehension of the molecular mechanisms behind GBM immune escape (IE).

Methods Protein chip analysis was performed to screen aberrantly expressed OMA1 protein in PD-1 inhibitor sensitive or resistant GBM. Herein, public databases and bioinformatics analysis were employed to investigate the OMA1 and PD-L1 relation. Then, this predicted relation was verified in primary GBM cell lines through distinct experimental methods. To investigate the molecular mechanism behind OMA1 in immunosuppression, a series of experimental methods were employed, including Western blotting, co-immunoprecipitation (Co-IP), mass spectrometry (MS), immunofluorescence, immunohistochemistry, and qRT-PCR.

Results Our findings revealed that OMA1 competitively binds to HSPA9 to induce mitophagy and mediates the IE of GBM. Data from TCGA indicated a significant correlation between OMA1 and immunosuppression. OMA1 promoted PD-L1 levels in primary cells from patients with GBM. Next, the results of Co-IP and MS conducted on GBM primary cells revealed that OMA1 interacts with HSPA9 and induces mitophagy. OMA1 promoted not only cGAS–STING activity by increasing mitochondrial DNA release but also PD-L1 transcription by activating cGAS–STING. Eventually, OMA1 has been found to induce immune evasion in GBM through its regulation of PD-1 binding and PD-L1 mediated T cell cytotoxicity.

Conclusions The OMA1/HSPA9/cGAS/PD-L1 axis is elucidated in our study as a newly identified immune therapeutic target in GBM.

BACKGROUND

Glioma represents the prevailing primary malignant neoplasm within the central nervous system tumors, with glioblastoma (GBM) exhibiting the most severe degree of malignancy and the worst prognosis for

WHAT IS ALREADY KNOWN ON THIS TOPIC

⇒ Overexpression of OMA1 in tumor tissues is associated with a poor prognosis in many tumors. Nevertheless, recent studies have mainly focused on the effect of OMA1 on cell metabolism while largely ignoring its immune-modulation function.

WHAT THIS STUDY ADDS

⇒ OMA1 inhibited the formation of IP3R/HSPA9/VDAC1 complex by competitively binding with IP3R to HSPA9, resulting in the blockage of mitochondrial tricarboxylic acid cycle. The impaired mitochondrial function will promote mitophagy, thereby increasing mitochondrial DNA release, activating the cGAS–STING signaling pathway, and overexpressing programmed death receptor 1 ligand (PD-L1).

HOW THIS STUDY MIGHT AFFECT RESEARCH, PRACTICE, OR POLICY

⇒ These findings highlight that OMA1 is a specific PD-L1 positive regulator that hinders the cytotoxicity of CD8⁺ T cells. Targeting OMA1 may synergize with immune checkpoint blockade for glioma immunotherapy.

patients, as evidenced by a 5-year survival rate below 10%.^{1 2} In spite of the implementation of an extensive, conventional treatment regimen that encompasses surgical intervention, radiation therapy, chemotherapy, and TTF, patients are observed to have a median survival period of merely 12–14 months subsequent to the initial diagnosis.^{2 3} The imperative objective for clinical researchers is to identify efficacious treatment modalities and enhance the prognosis of patients.

Recently, the immunotherapy of glioma has received extensive attention, but there is no effective immunotherapy for GBM so far. Therefore, elucidating the underlying mechanism of glioma immune microenvironment regulation can provide new therapeutic strategies for GBM. Immunotherapy, especially

targeting programmed death receptor 1 (PD-1)/PD-1 ligand (PD-L1) for immune checkpoint blockade, has brought about significant transformations in the management of various tumors.⁴ However, the clinical effect of targeting PD-1/PD-L1 in patients afflicted with GBM is still limited. Most patients suffering from GBM exhibit resistance to pharmaceutical interventions that specifically target PD-1/PD-L1, except for a limited subset of patients who demonstrate a positive response to immunotherapeutic approaches using this pathway.⁵ The response to PD-1/PD-L1 blockade was found to be related to PD-L1 expression levels in tumor cells.^{6,7} Moreover, PD-L1 protein levels were found to be related to glioma grades, and higher tumor cell PD-L1 levels contribute to immune evasion in glioma patients.^{8,9} To enhance effective strategies for glioma immunotherapy, the mechanisms behind PD-L1 regulation require further investigation.

OMA1 is a metalloprotease situated within the inner mitochondrial membrane and encoded by the OMA1 gene. Studies have shown that OMA1 can be triggered and activated by exogenous stimuli or cellular stress. OMA1 possesses the ability to cleave and degrade substrate proteins, including but not limited to OPA1, DELE1, and PINK1, owing to its protease activity. This enzymatic action allows OMA1 to modulate the morphology and functionality of mitochondria, consequently leading to alterations in various cellular biological processes, thereby resulting in a range of disorders.^{10,11} The upregulation of OMA1 in neoplastic cells has a correlation to a significant enhancement in both its expression and activity. This upregulation contributes to excessive cell proliferation and expedites tumor initiation and progression through its governing of mitochondrial function and cellular metabolism.¹² In a study conducted by Thomas Langer and colleagues, it was observed that the integrated stress response, mediated by OMA1, plays a protective role toward ferroptosis in cases of mitochondrial cardiomyopathy.¹³ In GBM, further research is needed to understand how OMA1 affects immunosuppression, particularly PD-L1 expression.

Herein, our results indicated that OMA1 is related to immunosuppression and overexpressing PD-L1 in PD-1 inhibitor-resistant GBM. Further, we found that the expression of OMA1 was increased, which inhibited the formation of IP3R/HSPA9/VDAC1 complex by competitively binding with IP3R to HSPA9, resulting in the blockage of mitochondrial TCA cycle. The impaired mitochondrial function will promote mitophagy, thereby increasing mitochondrial DNA release, activating the cGAS-STING signaling pathway, and overexpressing PD-L1. PD-L1 is recognized by PD-1 of CD8⁺ T cells and contributes to immune escape (IE).

Materials and methods

Clinical samples

Surgical samples of GBM were obtained from Wuhan Union Hospital (Wuhan, China). Online supplemental table S1 provides details on the patient features. Each

patient signed an informed consent form before specimen collection. All patients had not received chemoradiotherapy before surgery. This research followed the Declaration of Helsinki, and the necessary ethical authorizations were acquired.

Cell culture and treatment

For the detailed extraction and culture methods of GBM primary cells, please refer to the previous article.^{14–16} All cells underwent short tandem repeat analysis and were consistently screened for mycoplasma contamination. For more detailed steps on extraction, culture, and passage of GBM primary cells, please refer to the supplementary materials.

Plasmids and siRNAs

GeneChem (Shanghai, China) synthesized the lentiviral overexpression plasmids for OMA1 and HSPA9, as well as the lentiviral knockdown plasmids for OMA1 and c-GAS. Online supplemental table S2 lists the used sequences of shRNAs and siRNAs. PCR was used to amplify and clone the truncated structure cDNAs of human OMA1 (NM_145243.5) into the pECMV-3xFLAG-C expression vector. For transient transfections, Lipofectamine 3000 from ThermoFisher Scientific in the USA was used per the protocols. Subsequently, colonies expressing cells were chosen by applying 2 mg/mL puromycin for stable expression.

Western blotting (WB) and antibodies

Our previous studies published the related protocol details.^{14–17} Online supplemental table S3 provides details on all antibodies. For more detailed experimental procedures, please refer to the supplementary material.

Nuclear and cytoplasmic extraction, RNA extraction, and qRT-PCR

An RNA purification kit (AM1921, Thermo Fisher Scientific) was used to separate nuclear and cytoplasmic RNA. The total RNA extraction from tissues or cell lines was conducted through Trizol (Takara, Otsu, Japan) per the protocols. With SYBR Green premix Pro Taq HS qPCR Kit (AG11728, Accurate Biotechnology, Hunan, China), the reverse transcription of 1 µg of total RNA into cDNA was performed using Evo M-MLV RT Kit. Real-time PCR reactions were carried out using the BioRad system (BioRad, USA). The internal reference GAPDH was employed to normalize the RT-qPCR results, calculating the relative expression via the $2(-\Delta\Delta CT)$ method. Online supplemental table S4 lists the primer sequences.

Transmission electron microscopy

Briefly, GBM primary cells were plated in T25 culture flasks and treated for 48 hours with different treatments. After centrifugation and precipitation, cells are collected. The cells went through resuspension in IEM fixative followed by fixation at 4°C for preservation. An electron microscope (Hitachi, HT7700, Japan) was used to obtain the images.

Bioinformatics analysis

The TCGA (<https://cancergenome.nih.gov/>) was accessed to download transcript data of glioma samples and clinical information while accessing the Genotype-Tissue Expression (<https://gtexportal.org/home/>) to download the transcript data of normal brain tissues.¹⁸ For more detailed experimental procedures, please refer to the supplementary material.

Co-immunoprecipitation (Co-IP)

We conducted Co-IP assays, as reported earlier.^{14 15 19} We first enriched mitochondrial proteins before performing immunoprecipitation to study the interaction between OMA1 and HSPA9. In brief, Protein A+G magnetic beads were used to hatch the indicated cell lysates for a whole night at 4°C with specific primary antibodies. Employing the corresponding antibodies, the immunocomplexes were then analyzed via immunoblotting after being rinsed with lysis buffer. Online supplemental table S3 provides detailed information on the antibodies used herein.

Determination of total cellular ATP

Aspirate the culture medium, add lysis liquid at a ratio of 200 μ L to each well of the 6-well plate (equivalent to 1/10 of 2 mL of cell culture medium), and lyse the cells. When lysing cells, in order to fully lyse them, you can use a pipette to repeatedly pipet or shake the culture plate to fully contact the lysis solution and lyse the cells. Normally cells lyse immediately after contact with the lysis buffer. After lysis, centrifuge at 12 000g for 5 min at 4°C, and take the supernatant for subsequent determination. Next, strictly follow the instructions of the ATP Assay Kit (YT361) to prepare the measurement of the standard curve, the preparation of the ATP detection working solution, and the measurement of the ATP concentration. For more detailed experimental procedures, please refer to the supplementary material.

Immunofluorescence (IF) and immunohistochemistry (IHC) staining

The study performed IF and IHC assays, as reported earlier.^{17 19 20} In brief, sectioned human or mouse tissue specimens were subjected to fixation in 4% paraformaldehyde, embedding in paraffin, and immunostaining with specific antibodies. The IF staining assays used 4% paraformaldehyde for 15 min at room temperature, 0.5% Triton X-100 for 10 min, and 5% BSA for 1 hour. Afterward, secondary antibodies with fluorine labels (1:200, Thermo Fisher Scientific) were applied. Then we stained nuclei with DAPI (C1002, Beyotime) using a fluorescent microscope (Nexcope NE930, Ningbo, China). Online supplemental table S3 lists the corresponding antibodies used herein.

Cell counting kit-8 (CCK-8) assay

The first step is to prepare the cell suspension. Cells were collected by trypsin digestion and centrifugation. The collected cells were resuspended in serum-containing medium, counted using a hemocytometer, and then

diluted to a single cell suspension of 5×10^3 – 5×10^4 cells/mL. The second step is to inoculate the cell suspension in a 96-well plate, 100 μ L per well, and design different concentration groups. Each concentration group can be designed with 3–6 duplicate wells and set up a blank group and a control group. The third step is to put the culture plate into the incubator and preculture it for about 24 hours (37°C, 5% CO₂). The fourth step is to add different concentrations of lentivirus to each well of the culture plate and place it in the incubator for 6–96 hours. Step 5: Add 10 μ L of CCK-8 solution to each well. After adding the reagent, gently shake the culture plate to help mix (to prevent errors caused by CCK-8 reagent sticking to the wall of the well). Try as much as possible during the adding process. Do not create bubbles to avoid affecting the OD value reading. Then put the culture plate into the incubator and incubate it for 1–4 hours. Finally, the absorbance (OD) at 450 nm was measured using a microplate reader.

Colony formation assay

To assess the colony formation ability of each cell line, the following experimental procedure was carried out. In short, cell plating, incubation, fixation, staining, colony counting and photography and replicate experiments. For more detailed experimental procedures, please refer to the supplementary material.

Confocal microscopy

The HBAD-EGFP-LC3 and HBAD-h-mito-dsRed adenoviral particles were obtained from HanBio (Shanghai, China). The cells were cultured for another 24 hours after infection with adenoviral particles. Following three PBS washes, the glioma cells were incubated at 37°C for 1 hour in the dark with 4% paraformaldehyde. After that, the sections were mounted with VECTASHIELD Antifade Mounting Medium containing DAPI (H-1200, Vector Laboratories, Burlingame, California, USA). As a final step, samples were imaged using a Nikon A1+/A1R⁺ confocal laser microscope (Nikon, Tokyo, Japan).

Xenograft model

In view of the advantages of fast reconstruction, high conversion rate, and low cost of the humanized mouse immune reconstitution model of PBMC, the authors used this model in this study to explore and verify the role of the main molecule OMA1 in tumor immunity. Briefly, following the random categorization into distinct groups, female NOG-dKO mice (aged 6–8 weeks, n=5/group) went through anesthesia. Subsequently, a suspension of 5 μ L GBM cells (5×10^6 cells) (with indicated treatment) was injected into the mouse brain with the stereotaxic device. Tumor size estimation was conducted using the formula $V=(D \times d^2)/2$, where D and d refer to the longest and shortest diameter, respectively. For more detailed experimental procedures, please refer to the supplementary material.

Statistical analysis

The study employed SPSS V.25.0 (SPSS, Chicago, Illinois, USA) and GraphPad Prism (V.8.0; GraphPad, La Jolla, California, USA) for performing all statistical analyses. For more detailed experimental procedures, please refer to the supplementary material.

RESULTS

OMA1 promotes GBM progression and is closely associated with prognosis

Clinically, we found that some patients with GBM are sensitive to PD-L1 inhibitors, while others are resistant. In order to further elucidate the molecular mechanism behind this phenomenon, we collected tumor samples from these patients and carried out primary isolation and culture. The protein chip technology was used to screen the differential proteins between the two. The heatmap shows the top 15 differentially expressed proteins in PD-1 inhibitor sensitive or resistant GBM (online supplemental figure S1A). Subsequently, we used methods such as bioinformatics analysis and the novelty of candidate molecules, and finally, we locked the research molecule OMA1. Then, the study used WB for validating OMA1 expression in PD-1 inhibitor-sensitive or resistant GBM, revealing that OMA1 was overexpressed in PD-1 inhibitor-resistant GBM (online supplemental figure S1B). From TCGA GBM database results, we found OMA1 was upregulated in glioma, was proportional to tumor grade, and was inversely proportional to the patient's prognosis (online supplemental figure S1C,D). Herein, about online supplemental figure S1D, we only use two standardized methods, FPKM and TPM, for quantitative grouping, and adopt different statistical assumptions. Currently, TPM is more recommended. These two pictures actually express the same meaning. Aiming to verify OMA1 biological function, we knocked down and overexpressed OMA1, respectively, followed by employing qRT-PCR and WB for validating the efficiency of knockdown and overexpression (online supplemental figure S1E). CCK-8, colony formation experiments, and EdU experiments all showed that overexpression of OMA1 (oeOMA1) promoted GBM proliferation while knocking down OMA1 had the opposite effect (figure 1A–C and online supplemental figure S2A–C). Similarly, animal experiments on intracranial orthotopic tumorigenesis of glioma showed that oeOMA1 promoted GBM growth while knocking down OMA1 had the opposite effect. The results of KI67 IF-staining on the tumor specimens of the above two groups of animals also confirmed the above results again (figure 1D and online supplemental figure S1F and S2D). The above results indicate that OMA1 can promote the progression of GBM.

OMA1 mediates IE in GBM

In order to further explore whether OMA1 can mediate the IE of GBM, we cocultured primary GBM cells overexpressing or knocking down OMA1 with CD8⁺ T cells *in vitro*. The number of surviving primary cells with OMA1

overexpressing increased, whereas the surviving number of GBM primary cells with OMA1 knockdown decreased (figure 2A and online supplemental figure S3A). Consequently, CD8⁺ T cell growth and IFN- γ , TNF- α , and Gzmb expressions were determined by employing flow cytometry and qPCR. The outcomes exhibited that CD8⁺ T cells exhibited lower TNF- α , IFN- γ , and Gzmb expression levels and proliferation in the oeOMA1 groups (figure 2B–E). However, the OMA1 knockdown groups showed that CD8⁺ T cells exhibited higher TNF- α , IFN- γ , and Gzmb expression levels and proliferation (online supplemental figure S3B–E). The following procedures were followed to establish an intracranial orthotopic tumor model in a nude mouse: The primary GBM cells were implanted orthotopically into the mouse brain while being subjected to various treatment conditions. Following a 15-day period, the activated CD8⁺ T cells that were isolated from healthy human peripheral blood were administered through the tail vein at intervals of 3 days, revealing that mice subjected to oeOMA1 injection showed a significantly increased tumor size more than the control. Yet, OMA1 knockdown groups showed that tumor size significantly decreased. As anticipated, the IF analysis of Ki-67 in the transplanted animal tumor samples revealed that the oeOMA1 groups exhibited a higher Ki-67 expression than the mice in the Vector groups. However, OMA1 knockdown groups showed weakened expression of Ki-67 (figure 2F,G and online supplemental figure S3F,G).

Furthermore, ELISA outcomes revealed that CD8⁺ T cells supernatants that were cocultured with GBM primary cells overexpressing OMA1 exhibited reduced IFN- γ , TNF- α , and Gzmb secretion levels, while the OMA1 knockdown groups exhibited the opposite effect (online supplemental figure S4A). Moreover, the IF of CD8 on the transplanted animal tumor samples in each group revealed that the proportion of CD8⁺ cells in the oeOMA1 groups was significantly lower than in the control. However, OMA1 knockdown groups showed higher expression of CD8 (online supplemental figure S4C).

OMA1 promotes tumor IE via mitophagy

Mitochondria are organelles that contribute to multiple functions, including energy metabolism, cell signal regulation, and apoptosis in eukaryotes.²¹ Mitophagy controls mitochondrial mass and maintains cellular homeostasis by selectively degrading excess or damaged mitochondria.^{22–23} Mitophagy is involved to a great extent in regulating immune-related diseases, including tumors,^{24,25} neurodegenerative diseases,^{26,27} and cardiovascular diseases.^{28,29} Interestingly, it has been reported that BNIP3L, a key protein of mitophagy, is highly expressed in glioma, so it is speculated that the mitophagy pathway is activated in glioma.^{30,31} Nevertheless, the mitophagy and tumor IE association remains unelucidated. Therefore, we wanted to explore whether mitophagy possesses a regulatory role in the process of OMA1 promoting IE in glioma.

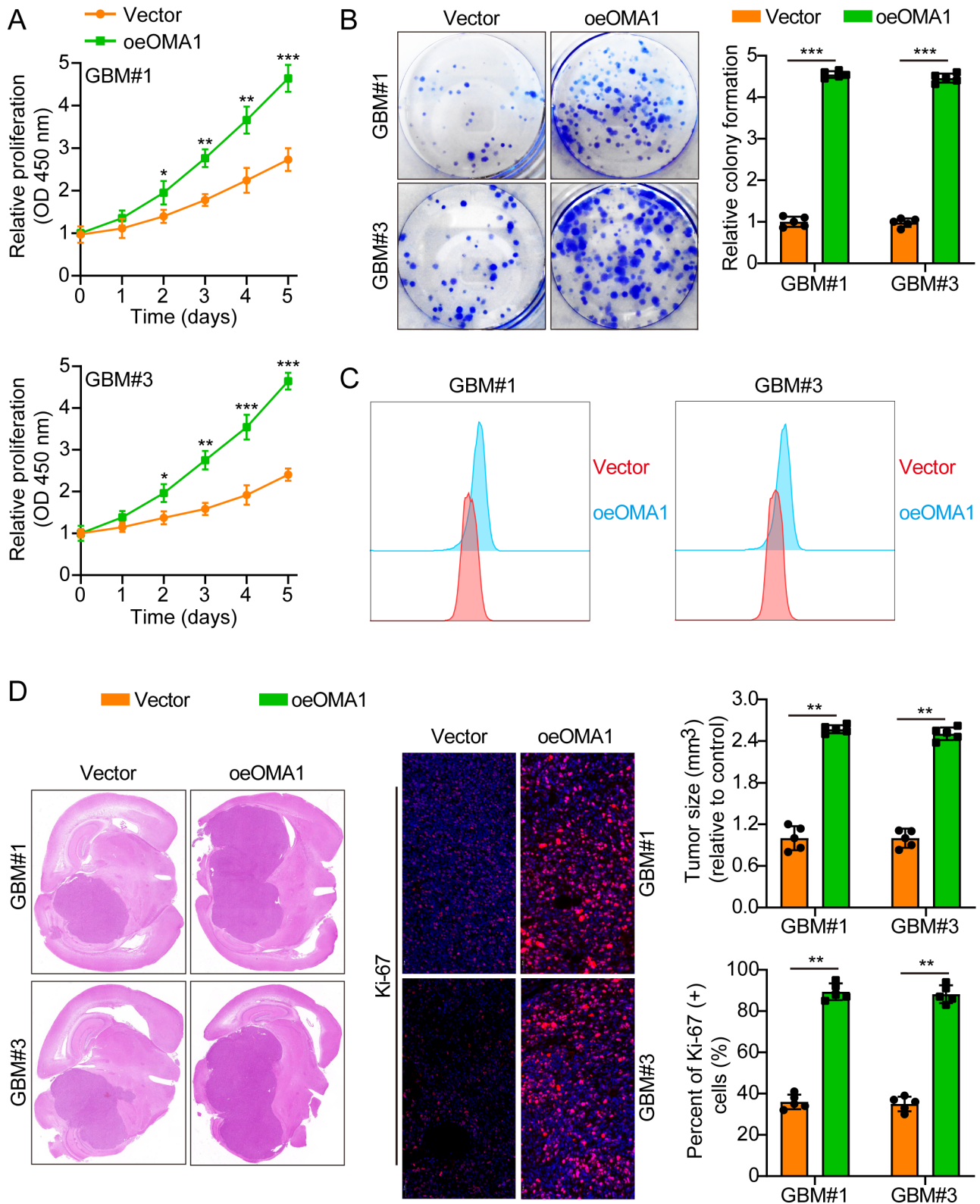


Figure 1 OMA1 promotes the growth of GBM. (A–C) The results of CCK-8, clone formation assays, and EdU assays all showed that oeOMA1 promoted the proliferation of GBM primary cells. The right side represents a typical histogram. (D) The results of animal experiments on orthotopic tumorigenesis of glioma also showed again that OMA1 promotes the intracranial growth of GBM. Representative Ki-67 immunofluorescent staining and corresponding histograms of intracranial tumor specimens of mice in various animal experiments (n=5). Scale bar, 50 μ m. The means \pm SDs are provided (n=5). *p<0.05, **p<0.01, and ***p<0.001 according to two-tailed Student's t-tests or one-way ANOVA followed by Dunnett tests for multiple comparisons. ANOVA, analysis of variance; CCK-8, cell counting kit-8; GBM, glioblastoma; oeOMA1, overexpression of OMA1.

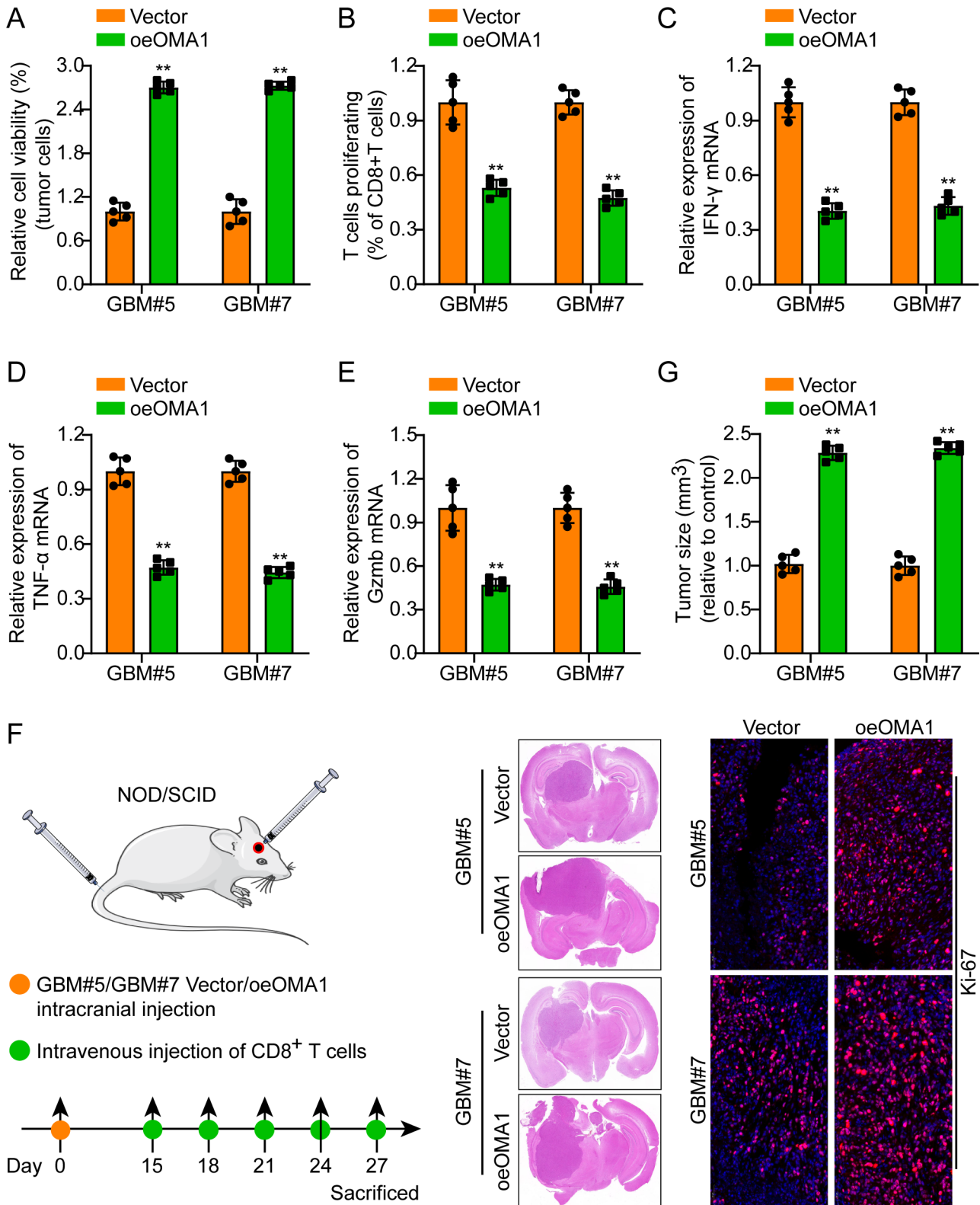


Figure 2 OMA1 promotes immune escape in GBM. (A) oeOMA1 significantly inhibited T cell-mediated tumor cell killing compared with Vector. (B–E) Flow cytometry and qPCR results indicated that CD8⁺ T cells cocultured with GBM primary cells overexpressing OMA1 showed lower proliferation and expression of IFN- γ , TNF- α , and Gzmb. (F) Schematic diagram of animal experiments. (G) Typical animal experiment tumor slices, Ki-67 IF pictures, and typical column chart in different groups. Scale bar, 50 μ m. The means \pm SDs are provided (n=5). *p < 0.05 and **p < 0.01 according to two-tailed Student's t-tests or one-way ANOVA followed by Dunnett tests for multiple comparisons. ANOVA, analysis of variance; GBM, glioblastoma; oeOMA1, overexpression of OMA1.

Next, in the GBM primary cells overexpressing OMA1, the mitophagy markers PINK1, p-Parkin, BNIP3, and BNIP3L were detected by WB, and the expressions were all increased. In addition, WB was employed for detecting the expression levels of marker proteins LC3-II/I of autophagy flow, and it was observed that the LC3-II/I ratio increased. Additionally, to further confirm the alterations in autophagy flux, the inhibition of lysosomal degradation by bafilomycin A1 should be employed (figure 3A). By combining TOM20 and LC3 fluorescent signals, OMA1 enhanced autophagosome-mitochondrion colocalization (figure 3B,C). PINK1/Parkin represents a key signaling pathway mediating mitophagy in mammals, and it is involved in autophagosome formation.³² After overexpressing OMA1, PINK1 and Parkin expression were detected. As shown, oeOMA1 enhanced PINK1, p-Parkin^{ser65}, and LC3 expressions in GBM primary cells (figure 3D). The Parkin translocation to mitochondria represents a well-known mitophagy hallmark.³³ Therefore, we proceeded to investigate this translocation in flubendazole-treated cells through analysis of cellular fractionations. Just like expectation, Parkin exhibited enrichment in the mitochondria fraction in oeOMA1 groups (figure 3E). Consistently, the aforementioned findings were additionally corroborated by the heightened level of PINK1 and Parkin colocalization in oeOMA1 groups (figure 3F). Based on these findings, OMA1 triggers mitophagy through PINK1/Parkin signaling in GBM.

Furthermore, we assessed the influences of OMA1 on the mitochondrial permeability transition pore (mPTP) opening in GBM primary cells. In comparison with the Vector groups, the oeOMA1 groups significantly decreased Calcein AM fluorescence intensity, indicating an accelerated rate of opening of mPTP (online supplemental figure S5A). Permeability in the mitochondria's outer membrane is often accompanied by morphological changes and dysfunction.³⁴ To assess OMA1-induced mitochondrial changes in GBM primary cells, we analyzed mitochondrial morphology, quantity, and function. MitoTracker Deep Red FM probe was used to stain GBM primary cells. It has been observed that the oeOMA1 groups significantly enhanced the number of mitochondria displaying ring-shaped structures in GBM primary cells more than in the control. This observation suggests the presence of mitochondrial fission or even fragmentation (online supplemental figure S5B). Additionally, mitochondrial DNA copy number was used to determine the relative mitochondrial number. Consequently, oeOMA1 decreased mtDNA copy number, suggesting mitochondrial loss (online supplemental figure S5C). Additionally, oeOMA1 enhanced mitochondrial fission (online supplemental figure S5D). In addition, oeOMA1 induced an increased ATP level and an increase in superoxide in GBM primary cells (online supplemental figure S5E,F). Of course, we also examined mitochondrial ATP energy production and total cellular ATP production. The results showed that overexpression of OMA1 reduced mitochondrial ATP energy production but increased total cellular

ATP energy production. This is also consistent with the metabolic characteristics of tumor cells. Normally differentiated cells mainly rely on oxidative phosphorylation of mitochondria to supply energy to cells, while most tumor cells rely on aerobic glycolysis. This phenomenon is called the "Warburg effect." That is to say, tumor cells rely on aerobic glycolysis that occurs in the cytoplasm for energy. To further clarify OMA1 promotes tumor IE through mitophagy. We added the mitophagy inhibitor Brefeldin A to the coculture system of OMA1-overexpressing GBM primary cells and CD8⁺ T cells and found that Brefeldin A could reduce OMA1-mediated IE (figure 4A-G).

Although the reduction in Calcein AM fluorescence can indicate changes in mitochondrial membrane permeability, it also reflects decreased cell viability and apoptotic features. However, we assert that cells under this condition exhibit higher activity and increased proliferative capacity. According to the literature, OMA1 is a regulator of cell apoptosis, with its overexpression promoting the release of cytochrome c. Herein, we used WB to detect the expression of OMA1 in normal astrocytes (NHA) and glioma cell lines (T98G, LN-18, LN-229, A-172 and U-87). The results showed that compared with astrocytes, OMA1 was highly expressed in glioma cell lines (online supplemental figure S6A). In addition, as the tumor grade increases, the expression level of OMA1 also increases (online supplemental figure S6B). We selected T98G, which has a low expression of OMA1, as the cell line that overexpresses OMA1, and LN-229, which has a high expression of OMA1, as the cell line that knocks down OMA1. The results showed that knocking down OMA1 inhibited the expression of cytochrome c while overexpressing OMA1 promoted the expression of cytochrome c (online supplemental figure S6C). Because cGAS/STING is required, we also observed type I IFN in culture (online supplemental figure S6D). Besides, we have conducted experiments to investigate whether STING impacts CD8 recruitment, particularly through the CXCL10-CXCR3 pathway. Our findings indicate that compared with the control group, adding CXCL10 to the lower chamber significantly promoted the migration of CD8⁺ T cells into the lower chamber through the Transwell membrane. The data suggest a notable influence of STING on CD8 recruitment, with a specific involvement of the CXCL10-CXCR3 pathway (online supplemental figure S6E). Of course, the main effect of OMA1 targeting is an effect on proliferation so it is very difficult to claim that immune system have are role in the delay in tumor growth. We will perform and supplement these data on syngeneic models like GL261. Specifically, we will perform targeting experiments of OMA1 in WT and RAG mice to confirm the current hypothesis. Such experiments will provide us with deeper insights into a more comprehensive understanding of the impact of OMA1 targeting on tumor growth, thereby strengthening our study conclusions. Animal experimental results show that overexpression of OMA1 promotes tumor growth while knocking down OMA1 inhibits tumor growth (online

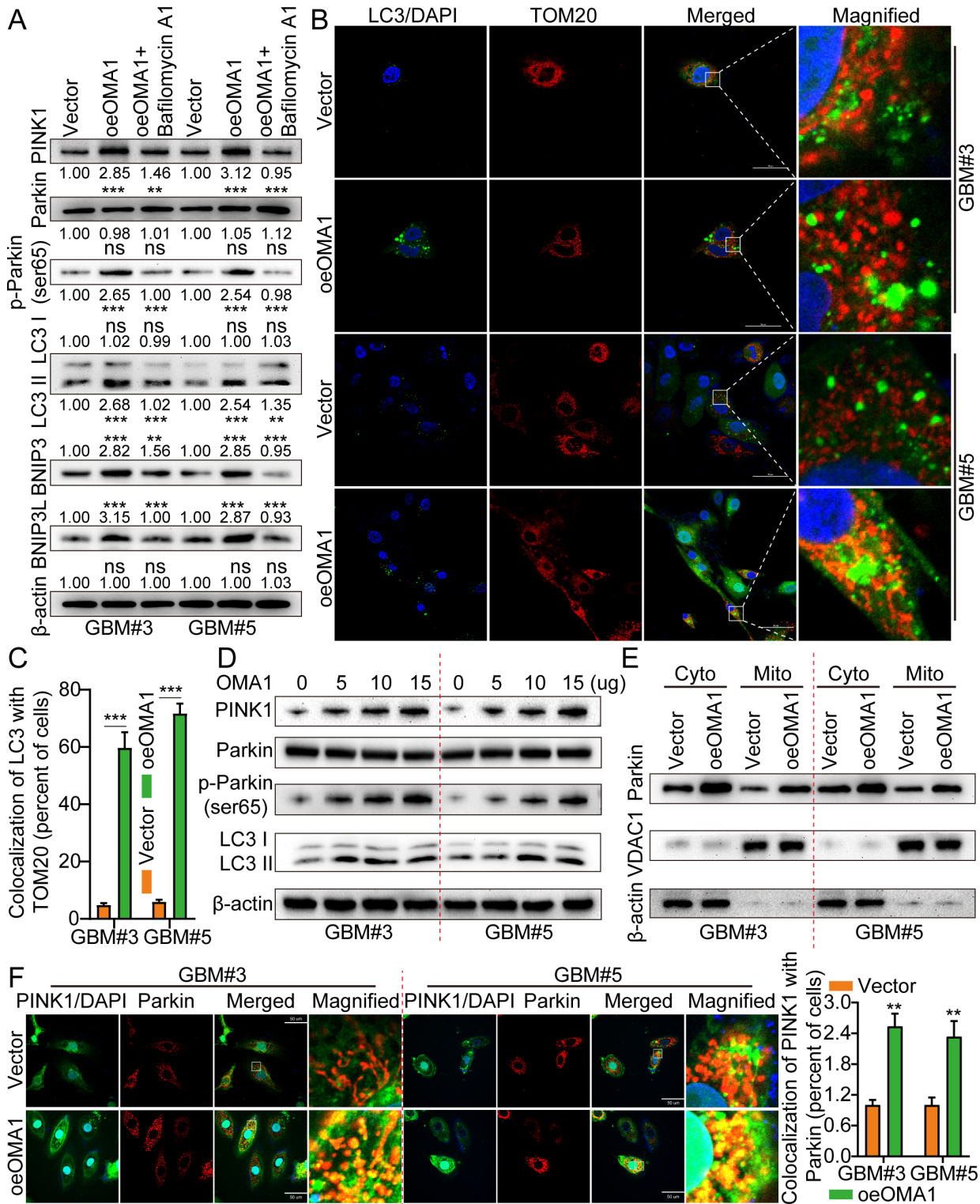
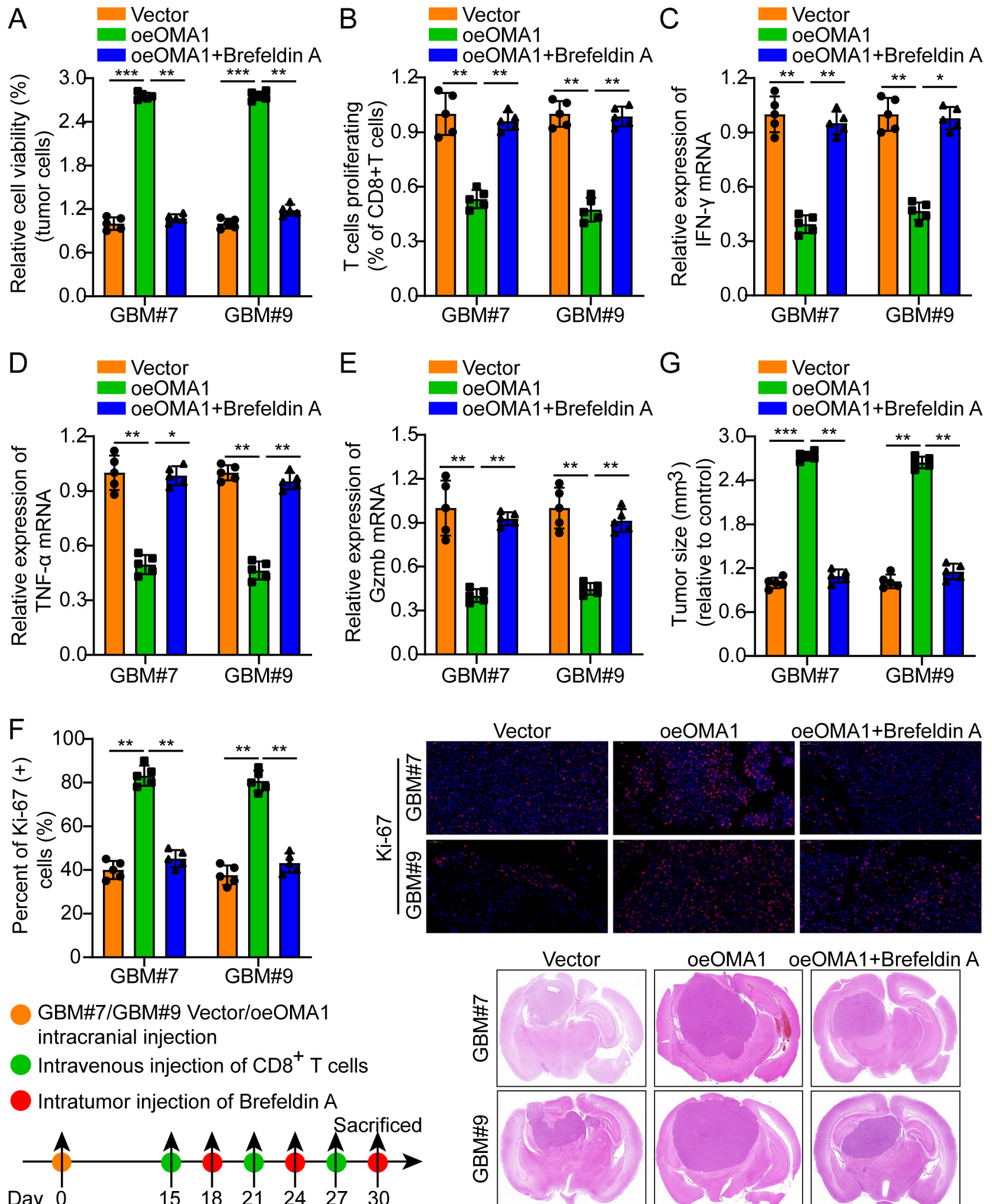


Figure 3 OMA1 promotes mitophagy via PINK1/Parkin signaling. (A) The results of WB experiments showed that oeOMA1 promoted the expression of PINK1, p-Parkin^{ser65}, LC-3, BNIP3, and BNIP3L. (B, C) The autophagosomes are labeled by LC3 (green fluorescence) protein, and the mitochondria are labeled by TOM20 (red fluorescence) protein. The number of colocalized LC3 and TOM20 was quantified. Scale bar, 50 μ m. (D) WB of PINK1, Parkin, p-Parkin^{ser65}, and LC3 in GBM primary cells treated with the indicated concentrations of OMA1 for 24 hours. (E) WB of Parkin in the cytosolic and mitochondrial fractions of GBM primary cells treated with or without oeOMA1 for 24 hours. β -Actin (cytoplasmic fraction) and VDAC1 (mitochondrial fraction) were used as the loading controls. (F) Colocalization of PINK1 (green fluorescence) protein and Parkin (red fluorescence) protein in GBM primary cells following oeOMA treatment or not. The number of colocalized PINK1 and Parkin was quantified. Scale bar, 50 μ m. The means \pm SDs are provided (n=3). **p<0.01 and ***p<0.001 according to two-tailed Student's t-tests or one-way ANOVA followed by Dunnett tests for multiple comparisons. ANOVA, analysis of variance; GBM, glioblastoma; NS, not statistically significant; oeOMA1, overexpression of OMA1; WB, Western blotting.



supplemental figure S6F,G). This study shows that OMA1 can effectively promote the intracranial growth of mouse GL261 glioma cells by inhibiting the infiltration of CD8⁺ T cells into the tumor microenvironment and weakening the toxicity of CD8⁺ T cells. When anti-CD8 monoclonal antibodies (A2102) were used to eliminate CD8⁺ T cells in mice, the tumor-promoting effect of OMA1 disappeared, proving that OMA1 relies on CD8⁺ T cells to exert its tumor-promoting effect in tumor immunotherapy (online supplemental figure S6H).

OMA1 competitively binds HSPA9 to inhibit the IP3R/HSPA9/VDAC1 complex and mediate mitophagy

For further exploration of the specific molecular mechanism behind OMA1 activating mitophagy, we performed Co-IP combined mass spectrometry (MS) experiments in GBM primary cells overexpressing OMA1 and found a series of proteins that bind to OMA1, among which HSPA9 caught our attention (figure 5A). Studies have reported that HSPA9 can form a complex with IP3R and VDAC1 to participate in the Ca²⁺ transport between the endoplasmic reticulum and mitochondria, which is crucial for the maintenance of mitochondria's normal function.³⁵ Mitophagy removes aging and dysfunctional mitochondria.²² Therefore, we speculate that the combination of OMA1 and HSPA9 interferes with the formation of IP3R/HSPA9/VDAC1 complex, impairs the normal function of mitochondria, and promotes mitophagy to clear damaged mitochondria. To verify this conjecture, we first proved that OMA1 could bind HSPA9 through Co-IP experiments (figure 5B). Laser confocal results showed that OMA1 and HSPA9 colocalize in the cytoplasm (figure 5C). Additionally, the Co-IP results indicated that oeOMA1 weakened the binding ability of HSPA9 to IP3R and VDAC1 (figure 5D). Knockdown of HSPA9 in control GBM primary cells simulated OMA1 competitively inhibiting the IP3R/HSPA9/VDAC1 complex and found that the expression of mitophagy markers PINK1, p-Parkin^{ser65}, LC-3, BNIP3, and BNIP3L increased, suggesting that OMA1 competitively combined with HSPA9 to inhibit IP3R/HSPA9. The HSPA9/VDAC1 complex promotes mitophagy (figure 5E).

Based on the secondary structure predicted with the InterPro (<http://www.ebi.ac.uk/interpro/>), PDB (<https://www.rcsb.org/>), and Pfam (www.pfam.org) databases, three OMA1 truncations were created for validating its binding to HSPA9. Co-IP assays provided evidence that the binding sequences specific to HSPA9 were found within the 168–354 aa region (A1) of OMA1 protein (online supplemental figure S7A). Once the binding series has undergone mutation (Δ OMA1), we employed WB to assess the autophagy-related molecule expressions in the context of OMA1 overexpression (oe Δ OMA1), revealing that mitophagy-related molecule (PINK1, p-Parkin, BNIP3, and BNIP3L) expression levels did not change significantly (online supplemental figure S7B). In addition, we also used PCR and WB to verify the overexpression efficiency of HSPA9 (online

supplemental figure S7C). Of course, we also confirm the precise region where HSPA9 binds to OMA1 (online supplemental figure S8A), mutate their binding sites and use WB to repeatedly verify the changes in mitophagy-related proteins after knocking down HSPA9 with mutated binding sites. As expected, there was no significant change in mitophagy-related proteins after knocking down HSPA9 with a mutated binding site (online supplemental figure S8B). Of course, we also performed IHC testing to detect the expression of PDL1 and OMA1 at different levels of Glioma (online supplemental figure S8C). Besides, the functional experiment results also indicated that oe Δ OMA1 failed to promote the IE of GBM (online supplemental figure S9A–G).

To further demonstrate that OMA1 competes with HSPA9 to mediate mitophagy. First, we examined mitochondrial components (including Mitofusin-2, SOD2, VDAC1, COX IV, and TOM20) by WB in primary GBM cells overexpressing OMA1. The results showed a dose-dependent decrease in these proteins (online supplemental figure S10A). The maintenance of mitochondrial integrity is achieved through the regulation of a delicate equilibrium between the mechanisms of fission and fusion.³⁶ Our previous experimental results also proved that OMA1 can promote mitochondrial fission (online supplemental figure S5). We found that oeOMA1 increased p-DRP1Ser616 in GBM primary cells (online supplemental figure S10A). This finding supports the hypothesis that Drp1 phosphorylation at the Ser616 site enhances its mitochondrial translocation, thereby inducing mitochondrial fission. Subsequently, an investigation was conducted to determine the significance of HSPA9 in the process of OMA1-induced mitophagy in GBM. Overexpression of OMA1 and simultaneous overexpression of HSPA9 (oeHSPA9) in GBM primary cells. HSPA9 overexpression significantly reduced OMA1-induced colocalization of the autophagosome within the mitochondria (online supplemental figure S10B). Similarly, the utilization of WB and IF analysis demonstrated that oeHSPA9 resulted in a reduction in PINK1 and Parkin expressions when subjected to OMA1 treatment (online supplemental figure S10C,D).

OMA1 upregulates PD-L1 on the GBM surface by promoting mitophagy and activating the mtDNA–cGAS–STING pathway

Studies have reported that mitophagy can promote mitochondrial DNA release into the cytoplasm and activate the cGAS–STING pathway.^{37, 38} Accumulating evidence has indicated that the cGAS–STING pathway contributes significantly to tumor immunity.³⁹ In order to verify whether OMA1 activates the mtDNA–cGAS–STING pathway through mitophagy, we performed cytoplasmic isolation in GBM primary cells overexpressing OMA1 and detected the mtDNA marker genes D-LOOP, CytB, and ND4 in the cytoplasm by qPCR. The expression was found to be significantly increased. However, the expression of D-LOOP, CytB, and ND4 could be downregulated after adding the mitophagy inhibitor Mdivi-1 (figure 6A).

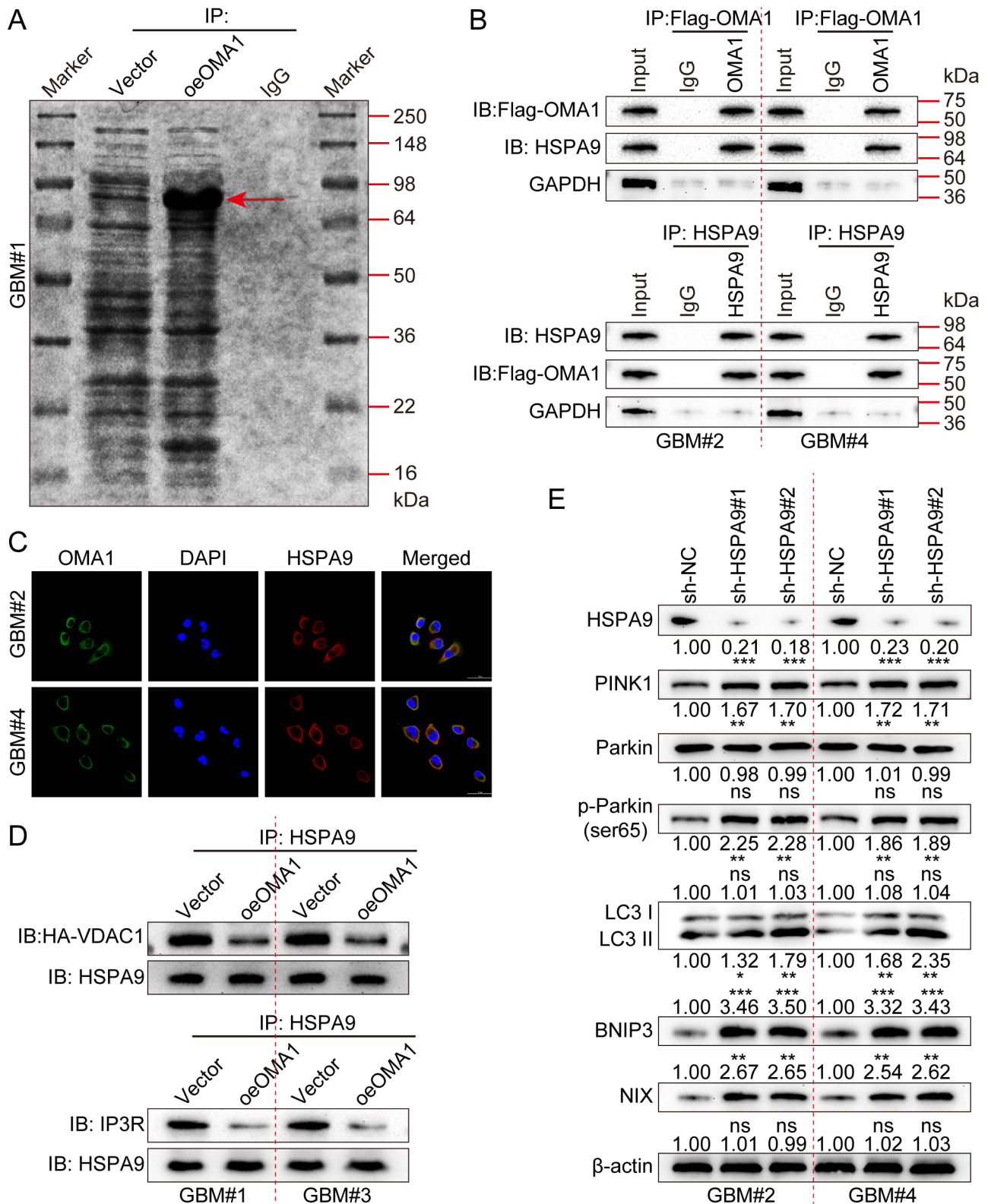


Figure 5 OMA1 competitively binds HSPA9 to inhibit the IP3R/HSPA9/VDAC1 complex and mediate mitophagy. (A) Identification of OMA1-binding proteins by WB and MS. (B) Using Co-IP to clarify that OMA1 could directly bind HSPA9. (C) The results of laser confocal experiments showed that OMA1 and HSPA9 colocalized in the cytoplasm of GBM primary cells. (D) The results of Co-IP experiments showed that oeOMA1 weakened the binding ability of HSPA9 to IP3R and VDAC1. (E) WB of PINK1, p-Parkins65, LC-3, BNIP3, and BNIP3L in GBM primary cells treated with the indicated treatment. The means±SDs are provided (n=3). *p<0.05, **p<0.01, and ***p<0.001 according to two-tailed Student's t-tests or one-way ANOVA followed by Dunnett tests for multiple comparisons. ANOVA, analysis of variance; Co-IP, co-immunoprecipitation; GBM, glioblastoma; MS, mass spectrometry; NS, not statistically significant; oeOMA1, overexpression of OMA1; WB, Western blotting.

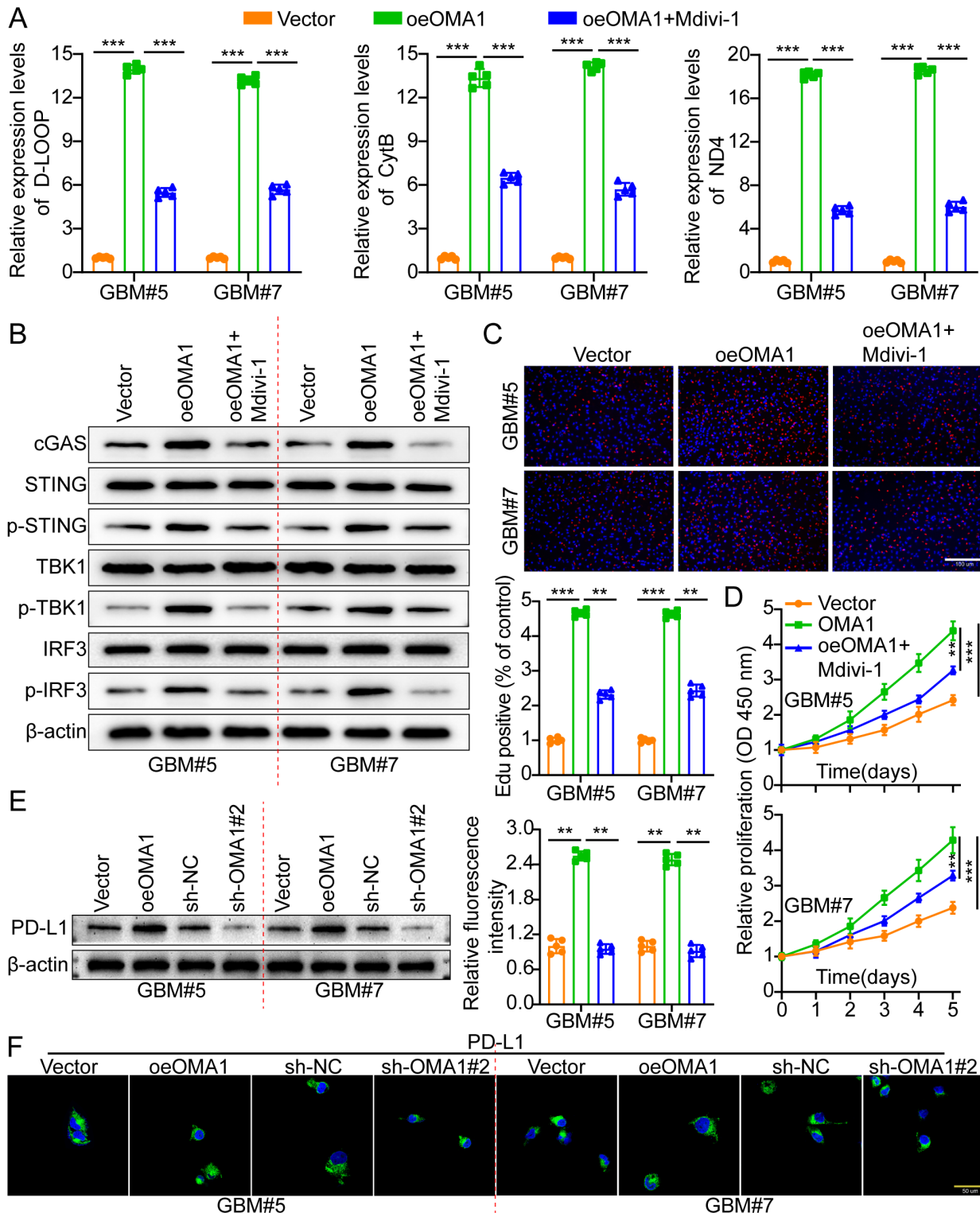


Figure 6 OMA1 promotes mitophagy and activates the mtDNA-cGAS-STING pathway to upregulate PD-L1 on the GBM surface. (A) oeOMA1 significantly promoted the expression of mtDNA marker genes D-LOOP, CytB, and ND4 in the cytoplasm by qPCR. However, the mitophagy inhibitor Mdivi-1 could rescue the above phenomenon. (B) oeOMA1 significantly enhanced the expression of cGAS, p-STING, p-TBK1, and p-IRF3 by WB. However, the mitophagy inhibitor Mdivi-1 could rescue the above phenomenon. (C, D) The results of CCK-8 and EdU assays indicated that oeOMA1 promoted the proliferation of GBM primary cells. However, the mitophagy inhibitor Mdivi-1 could rescue the above phenomenon. The bottom represents a typical histogram. (E, F) The results of WB and IF showed that overexpression of OMA1 promoted the expression of PD-L1, while knockdown of OMA1 inhibited the expression of PD-L1. The means \pm SDs are provided (n=5). **p<0.01 and ***p<0.001 according to two-tailed Student's t-tests or one-way ANOVA followed by Dunnett tests for multiple comparisons. ANOVA, analysis of variance; GBM, glioblastoma; IF, immunofluorescence; NS, not statistically significant; oeOMA1, overexpression of OMA1; PD-L1, programmed death receptor 1 ligand; WB, Western blotting.

Further, the key molecules of the c-GAS–STING pathway (cGAS, STING, p-STING, TBK1, p-TBK1, IRF3, p-IRF3) were detected by WB, and the pathway was found to be activated. Yet Mdivi-1 can downregulate the phosphorylation level of key molecules in this pathway (figure 6B). The results of Edu and CCK-8 cell function experiments also showed again that oeOMA1 significantly enhanced primary GBM cell proliferation. However, Mdivi-1 could weaken OMA1 capability to promote primary GBM cell proliferation (figure 6C,D), suggesting that OMA1 activates the cGAS–STING pathway dependent on the mitophagy pathway. To further verify that OMA1-activated cGAS–STING pathway is related to its activated IE, we simultaneously knocked down c-GAS in GBM primary cells overexpressing OMA1. The key molecule PD-L1, which mediates tumor IE, was detected in GBM primary cells overexpressing/knocking down cGAS by WB and IF, and PD-L1 expression was also increased/decreased (figure 6E,F). We verified c-GAS knockdown efficiency by WB and qPCR (online supplemental figure S11A). In addition, we simultaneously knocked down c-GAS in primary GBM cells overexpressing OMA1 and cocultured them with CD8⁺ T cells in vitro, revealing again that OMA1 promoted IE of GBM. However, the knockdown of c-GAS could weaken the ability of OMA1 to promote the IE of GBM (figure 7A–G). Interestingly, the TCGA database analysis showed that OMA1 expression is directly proportional to PD-L1 (online supplemental figure S11B) and inversely proportional to CD8⁺ T cell contents (online supplemental figure S11C).

Knockdown of OMA1 combined with PD-1 inhibitor can significantly inhibit the growth of GBM

In order to further demonstrate that OMA1 mediates GBM IE by overexpressing PD-1, we conducted the following experiments. First, we selected two primary GBM cell lines with high expression of OMA1 and resistance to PD-1 inhibitors, namely GBM#6 and GBM#8. Then we cocultured primary GBM cells knocking down OMA1 with CD8⁺ T cells in vitro and divided into whether to add PD-1 inhibitors in the medium. The results are completely consistent with the previous conclusions. The surviving number of GBM primary cells with OMA1 knockdown decreased. Consequently, CD8⁺ T cell growth and IFN- γ , TNF- α , and Gzmb expressions were determined by employing flow cytometry and qPCR. The outcomes exhibited that CD8⁺ T cells exhibited higher TNF- α , IFN- γ , and Gzmb expression levels and proliferation in the OMA1 knockdown groups (sh-OMA1#2+PBS vs. sh-NC+PBS). Interestingly, PD-1 inhibitors can significantly promote the biological functions mediated by knockdown of OMA1 (sh-OMA1#2+PD-1 inhibitor vs sh-OMA1#2+PBS). In addition, we demonstrated again through cell line functional experiments that primary GBM cells with high expression of OMA1 are indeed resistant to PD-1 inhibitors (sh-NC+PBS vs sh-NC+PD-1 inhibitor) (figure 8A and online supplemental figure S12A). Additionally, we performed apoptosis and colony formation

experiments, and the results showed that knocking down OMA1 can promote tumor cell apoptosis and inhibit proliferation (sh-OMA1#2+PBS vs sh-NC+PBS). Interestingly, PD-1 inhibitors can significantly enhance the biological functions mediated by knockdown of OMA1 (sh-OMA1#2+PD-1 inhibitor vs sh-OMA1#2+PBS). In addition, we demonstrated again through the two functional experiments that GBM primary cells with high expression of OMA1 are indeed resistant to PD-L1 inhibitors (sh-NC+PBS vs sh-NC+PD-1 inhibitor) (figure 8B and online supplemental figure S12B).

The following procedures were followed to establish an intracranial orthotopic tumor model in a nude mouse: GBM primary cells under different treatment conditions (sh-NC and sh-OMA1#2) were orthotopically implanted into the mouse brain. Following a 15-day period, the activated CD8⁺ T cells that were isolated from healthy human peripheral blood were administrated through the tail vein every 6 days. After 18 days, PBS or PD-1 inhibitors were also administrated via the tail vein every 6 days, revealing that mice subjected to the sh-OMA1#2+PBS injection had a significantly decreased tumor size more than control groups (sh-NC+PBS). Yet, the knockdown of OMA1 combined with PD-1 inhibitor groups showed that tumor size significantly decreased (sh-OMA1#2+PD-1 inhibitor vs sh-OMA1#2+PBS). Just like expectations, the IF of Ki-67 in the transplanted animal tumor samples revealed that control groups (sh-NC+PBS) exhibited enhanced Ki-67 expression more than the mice in the OMA1 knockdown groups (sh-OMA1#2+PBS). Additionally, sh-OMA1#2+PD-1 inhibitor groups showed weakened Ki-67 expression more than sh-OMA1#2+PBS. In addition, IHC staining of CD8 was conducted on the animal tumor specimens of the abovementioned groups, and corresponding scoring was performed. For the scoring rules, please refer to the previously published articles,^{15 17} and the results also confirmed the above conclusions again (figure 8C and online supplemental figure S12C).

Besides, we also recognize that cell lines may not be the most ideal GBM models and neurospheres would improve the quality of the paper. Owing to the profound effects of OMA1 on mitochondrial dynamics in GBM and the presence of distinct mitochondrial morphologies in GSCs, we investigated the functional roles of OMA1 and other mitophagy regulators in GSCs. First, we knocked down and overexpressed OMA1 in LN-229, T98G, and GBM primary cells, respectively, and observed the effect on the self-renewal capacity of glioma cells using spheroid formation and limiting dilution assays. Knockdown of OMA1 reduced the spheroiding ability of glioma cells compared with the control, whereas overexpression of OMA1 enhanced the spheroiding ability of glioma cells (online supplemental figure S13).

DISCUSSION

Tumor-induced immune suppression is by far the most extensively studied mechanism. There are two main

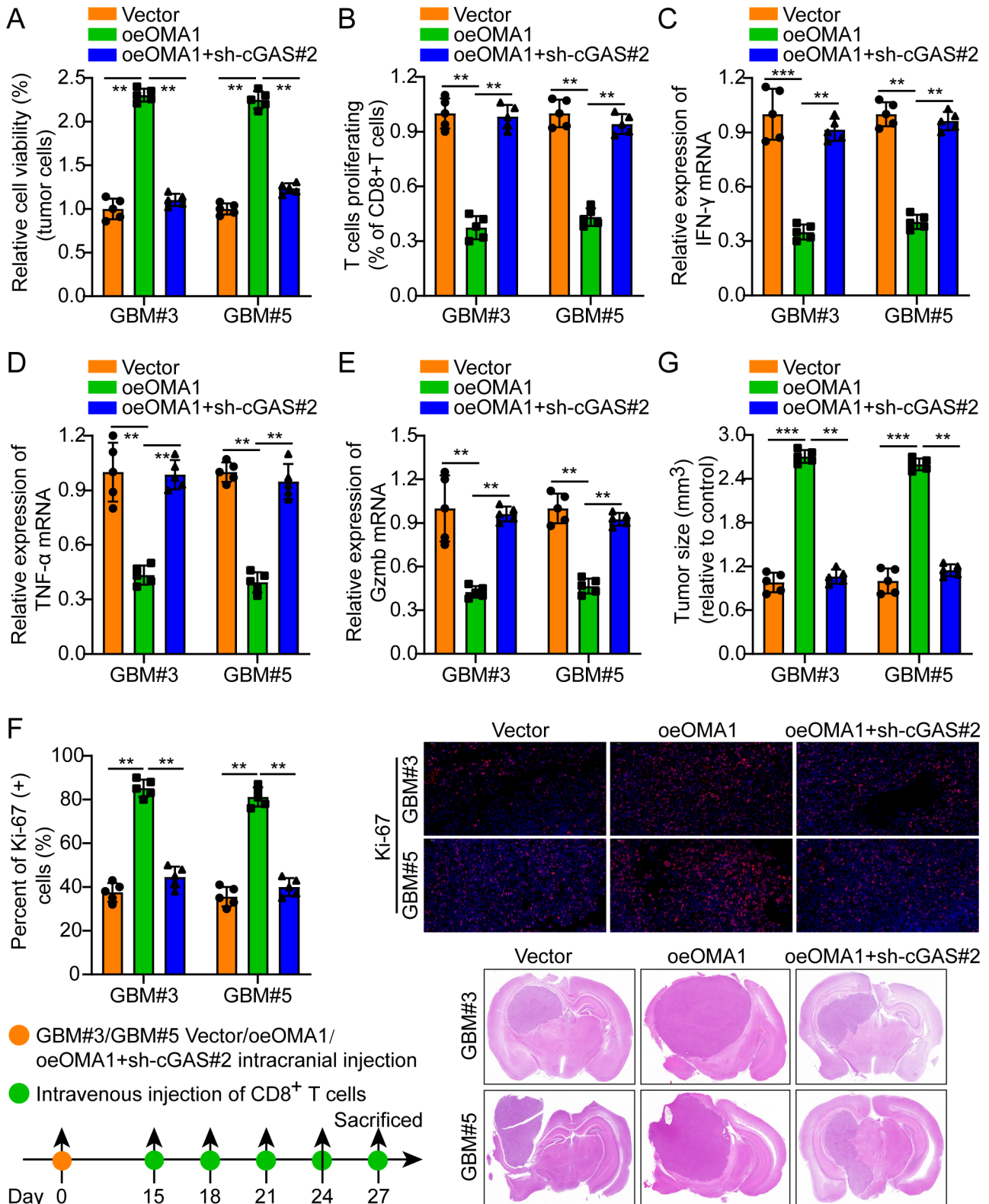


Figure 7 OMA1 promotes GBM immune escape through the mtDNA-cGAS-STING pathway. (A) oeOMA1 significantly inhibited T cell-mediated tumor cell killing compared with Vector. However, sh-cGAS#2 could rescue the above phenomenon. (B-E) Flow cytometry and qPCR results indicated that CD8⁺ T cells cocultured with GBM primary cells overexpressing OMA1 showed lower proliferation and expression of IFN- γ , TNF- α , and Gzmb. However, sh-cGAS#2 could rescue the above phenomenon. (F, G) Schematic diagram of animal experiments. Typical animal experiment tumor slices, Ki-67 IF pictures, and typical column charts in different groups. Scale bar, 50 μ m. The means \pm SDs are provided (n=5). **p<0.01 and ***p<0.001 according to two-tailed Student's t-tests or one-way ANOVA followed by Dunnett tests for multiple comparisons. ANOVA, analysis of variance; GBM, glioblastoma; oeOMA1, overexpression of OMA1.

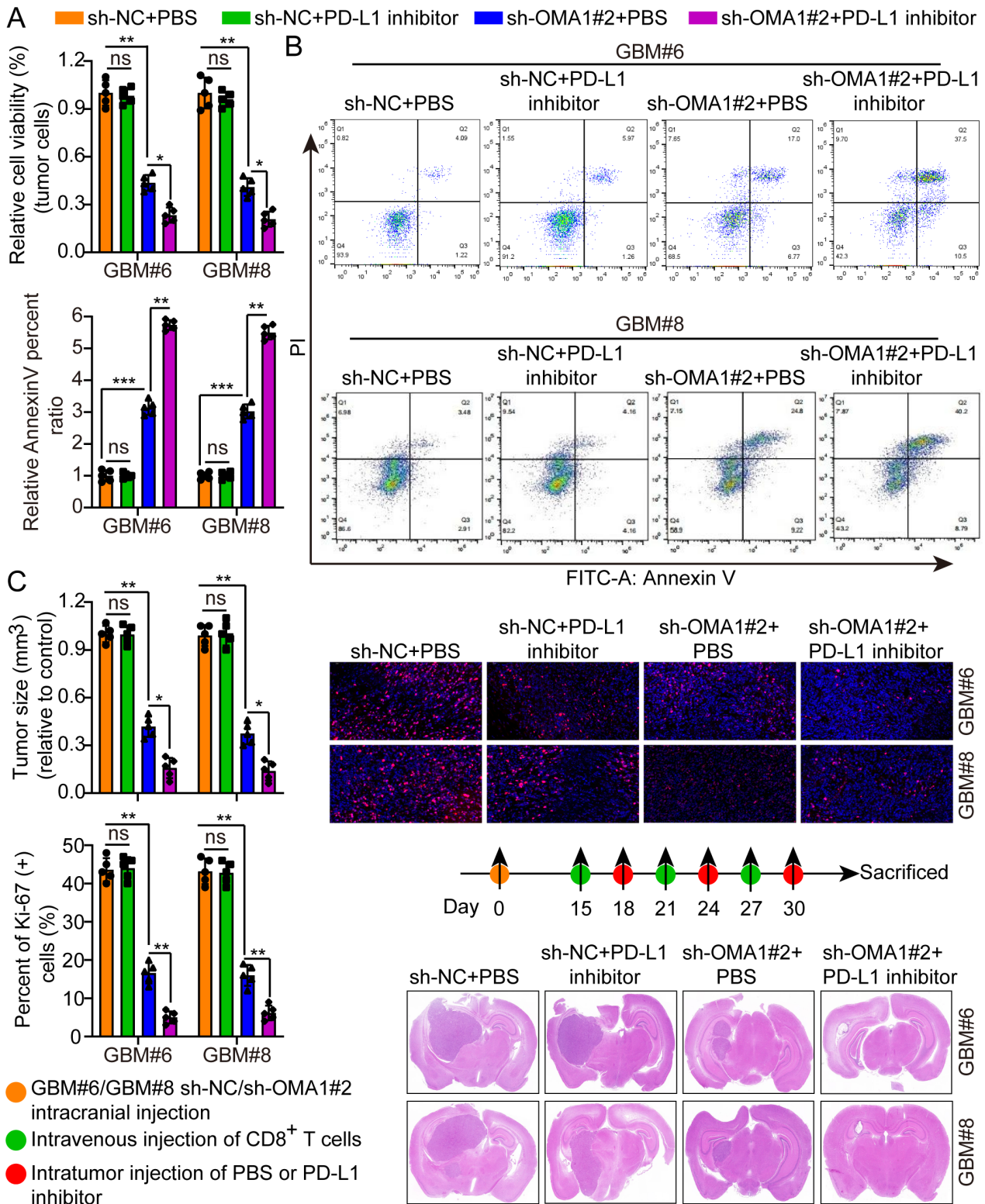


Figure 8 Knockdown of OMA1 combined with PD-1 inhibitor can significantly inhibit the growth of GBM. (A) OMA1 knockdown significantly enhanced T cell-mediated tumor cell killing compared with sh-NC+PBS. Furthermore, the combined use of PD-1 inhibitors could synergistically enhance the above functions. (B) OMA1 knockdown significantly promoted tumor cell apoptosis compared with sh-NC+PBS. Furthermore, PD-1 inhibitors can significantly enhance the biological functions mediated by knockdown of OMA1 (sh-OMA1#2+PD-1 inhibitor vs sh-OMA1#2+PBS). (C) Schematic diagram of animal experiments. Typical animal experiment tumor slices, Ki-67 IF pictures, and typical column chart between sh-NC+PBS, sh-NC+PD-1 inhibitor, sh-OMA1#2+PBS, and sh-OMA1#2+PD-1 inhibitor. Scale bar, 50 μ m. The means \pm SDs are provided ($n=5$). ** $p<0.01$ and *** $p<0.001$ according to two-tailed Student's t-tests or one-way ANOVA followed by Dunnett tests for multiple comparisons. ANOVA, analysis of variance; GBM, glioblastoma; NS, not statistically significant; PD-1, programmed death receptor 1.

ways of tumor-induced immunosuppression. The first is to induce immunosuppressive cells, including regulatory T cells, myeloid-derived suppressor cells, dendritic cells, and M2 macrophages, aiming at gathering around the tumor, secreting immunosuppressive factors, and inactivating cytotoxic T lymphocytes, thereby increasing immune tolerance of tumor cells.^{40–42} The second immunosuppressive mechanism entails overexpressing immunosuppressive molecules or their receptors, including PD-L1/PD-1, Galectin-9/Tim-3, IDO1, LAG-3, and cytotoxic T lymphocyte antigen-4 (CTLA-4). These molecules, commonly referred to as immune checkpoints (ICs), possess the ability to impede effector T lymphocyte activation, consequently resulting in tumor IE.⁴³ Moreover, ICs contribute significantly to immune homeostasis maintenance and autoimmunity prevention. The system comprises both stimulatory and inhibitory pathways, which are essential to maintain autoimmune tolerance and to govern immune response type, intensity, and duration. Under normal conditions, ICs enable the activation of immune system in order to initiate a defensive response toward infections and malignancies while simultaneously protecting normal tissues from potential harm resulting from this immune response. Nevertheless, the expression of certain IC proteins by malignant cells can dysregulate anti-tumor immunity and favor cancer cell growth and expansion.

As a form of treatment, tumor immunotherapy restores and maintains the body's normal antitumor immune responses in order to control and eliminate tumors. In many cases of cancer, immunotherapy has proven effective.^{44–46} In personalized medicine, tumor immunotherapy uses various essential proteins for improving or restoring the function of immune cells.^{47–48} Immunotherapy has been included in treatment guidelines for multiple cancers recently.^{49–50} PD-1, an immunoglobulin superfamily member, represents a crucial immunosuppressive molecule. Immunomodulation targeting PD-1 holds considerable importance in antitumor, anti-infection, antiautoimmune disorders, and organ transplant survival. Its ligand PD-L1 has the potential to function as a target, and the corresponding antibody can similarly fulfill this role. The binding of PD-1 ligand to its receptor PD-L1 or PD-L2 has the ability to hinder innate cytotoxic T cells from mounting an antitumor response through the inhibition of kinases contributing to T cell activation or by initiating T cell programmed death, enabling tumor cells to gain IE.^{51–52} Recently, some IC inhibitors were found to target PD-L1, CTLA-4, T cell immunoglobulin, and mucin domains containing molecule 3 (TIM-3) and programmed cell death protein 1 (PD-1) to enhance cytotoxic activity.⁵³ The utilization of antibodies for blocking the interaction between PD-L1 and the PD-1 receptor has exhibited significant enhancements in the survival rates of certain individuals diagnosed with lung cancer.^{54–55}

Studies have shown that the tumor microenvironment (TME) presents a highly immunosuppressive state, and high PD-1 expression has been found in tumor-infiltrating

lymphocytes of breast, prostate, ovarian cancers, as well as melanoma and among others. High PD-1 expression exhibits an association with tumor grade, size, lymph node metastasis, and distant metastasis, among others.^{56–57} PD-1 was found to be involved to a great extent in tumorigenesis. Additionally, PD-L1 is overexpressed in multiple tumor cells, and after combining with PD-1 molecules on the lymphocyte surface, it weakens the antitumor immune response of body, thereby enhancing tumor escape from the immune system.^{58–59} PD-L1 expression on the tumor cell surface may be a compensatory mechanism to cope with the TME. PD-1 protein consists of three parts: an N-terminal extracellular binding domain, a transmembrane domain, and a C-terminal cytoplasmic domain. The cytoplasmic domain comprises an immunoreceptor tyrosine-based switch motif (ITSM) and an immune receptor tyrosine-based inhibitory motif. When PD-L1 or PD-L2 binds to the PD-1 receptor on activated T cells, it can promote the tyrosine phosphorylation of the end of cytoplasmic domain of PD-1, and then recruit SHP-2 to ITSM, and finally, SHP2, it can dephosphorylate TCR-related proteins CD-3 ζ and ZAP70, and then disrupt a series of downstream signaling pathways: (1) inhibit the secretion of inflammatory factors TNF- α , IFN- γ , and IL-2; (2) inhibit PI3K/Akt, mTOR, activation of S6, Erk2, and other signaling pathways, while upregulating PTEN; (3) inhibit the metabolism of carbohydrates and amino acids, and promote the oxidation of fatty acids.⁶⁰ Moreover, tumor cell exosomes were found to carry PD-L1 on the surface, which can directly bind to T cells and inhibit T cell function.⁶¹

Mitophagy is mitochondria-specific autophagy, which contributes significantly to mitochondrial quality control by clearing damaged mitochondria and exhibits a close association with mitochondrial fusion and division. Mitochondria are highly dynamic structures. The rapid morphological adaptation of mitochondria is facilitated by the coordinated cycles of mitochondrial fusion and fission. These cycles also possess significant functions in governing the cell cycle, cellular immunity, apoptosis, and mitochondrial mass.^{62–63} The occurrence of dysmotility arises from an in-equilibrium in the processes of mitochondrial fusion and fission, leading to an inadequate supply of ATP or an excessive generation of ROS and NOS. These detrimental effects directly impair cellular integrity, consequently giving rise to various physiological abnormalities, including neurodegenerative disorders, cancer, and autoimmune diseases.⁶⁴ Mitophagy is a cellular process that specifically targets and eliminates mitochondria that are either damaged or no longer necessary. Mitophagy is a crucial element of the mitochondrial stress response and the maintenance of homeostatic regulation, as it serves as a regulatory mechanism for mitochondrial quality control.⁶⁵ Hence, in instances where the mitophagy process is compromised, there is a reduction in mitochondrial function or an occurrence of mitochondrial redundancy, which disrupts cellular homeostasis and contributes to the development

of associated disorders.⁶⁶ The mitophagy pathway can be categorized into three primary types, namely ubiquitin-mediated mitophagy, receptor-mediated mitophagy, and atypical mitophagy. According to the different receptors that mediate mitophagy, mitophagy is mainly divided into the following categories: (1) ATG-mediated yeast mitophagy, (2) Nix-mediated mitophagy, (3) Parkin and PINK-mediated mitophagy, (4) FUNDC1-mediated mitophagy, and (5) Bcl-rambo-mediated mitophagy.⁶⁶ The pathways that have received more extensive research attention include the PINK1–Parkin-mediated ubiquitin pathway and the FUNDC1 receptor-mediated pathway. In the PINK/Parkin pathway, following mitochondrial damage or the depletion of mitochondrial potential, PINK1 phosphorylates multiple target proteins, including ubiquitin. The PINK1 protein subsequently recruits Parkin, thereby amplifying the signal by ubiquitinating the receptor protein located on the surface of mitochondria. Receptor proteins are liable for recognizing ubiquitinated proteins, facilitating the mitochondrial generation of autophagosomes, and ultimately facilitating their degradation. The FUNDC1/BNIP3/NIX pathway involves the recognition of LC3 by mitochondrial receptor proteins, which facilitates the complementary binding of phagosomes and subsequently directs the selective removal of mitochondria through mitophagy, which is facilitated by the binding of mitochondrial outer membrane proteins FUNDC1, BNIP3, or NIX to LC3-II via their cytoplasmic LIR motifs.⁶⁷

Numerous variables exert an influence on the effectiveness of immunotherapy, encompassing changes in the TME, tumor-infiltrating lymphocytes (specifically CD8⁺ T cells related to treatment response), tumor-related macrophages, and some non-responsive patients. Activation of regulators (eg, PIK3 γ and PAX4), low percentage of PD-L1 and PD-1 expressing cells, tumor mutational burden, gain or loss of antigen-presenting molecules, genetic alterations in genes, or expression associated with drug resistance.⁶⁸ Developing pharmaceuticals that specifically target PD-1/PD-L1 star molecules is in the ascendant. In the follow-up research and development, in order to better benefit patients, there are many issues worthy of consideration by researchers. For example: Are there clinically detectable markers of efficacy? How to effectively combine anti-PD-1/PD-L1 drugs with existing chemotherapy, radiotherapy, surgery, and other treatment options? Can small molecule inhibitors of PD-1/PD-L1 be developed? How to solve the problem of drug efficacy being affected when DSB is combined with PD-L1 caused by radiotherapy and chemotherapy? How to reset the ability of anti-tumor immunity in the TME?

CONCLUSIONS

To conclude, we elucidated that OMA1 competitively binds to HSPA9 to promote mitophagy and activate the cGAS–STING pathway to mediate IE of GBM (figure 9). Additionally, we found that GBM with OMA1 deletion

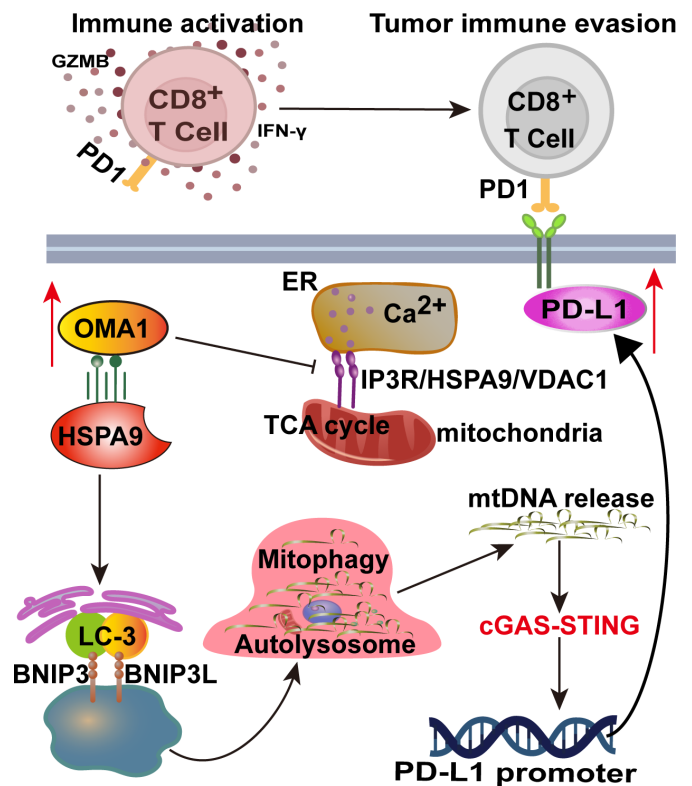


Figure 9 Mechanism diagram. In GBM, the expression of OMA1 was increased, which inhibited the formation of IP3R/HSPA9/VDAC1 complex by competitively binding with IP3R to HSPA9, resulting in the blockage of mitochondrial TCA cycle. The impaired mitochondrial function will promote mitophagy, thereby increasing the release of mitochondrial DNA, activating the cGAS–STING signaling pathway, and promoting the expression of PD-L1. PD-L1 is recognized by PD-1 of CD8⁺ T cells and plays a role in immune escape. GBM, glioblastoma; PD-L1, programmed death receptor 1 ligand.

or low expression is more sensitive to PD-L1 inhibitors; maybe in the future, we can develop OMA1 small molecule inhibitors combined with PD-L1 inhibitors to treat GBM.

X Rong Fu @furong

Acknowledgments We thank Home for Researchers editorial team (www.home-for-researchers.com) for language editing service.

Contributors WdZ, JR, QzC, and RF conceived and designed this study. WdZ, JR, and QzC performed the experiments. LhZ, KmX, KZ, and JjL analyzed the data. WdZ and RF wrote the manuscript. QzC and RF revised the manuscript. The author(s) read and approved the final manuscript. RF is responsible for the overall content as the guarantor.

Funding The Natural Science Foundation of Hubei, China (No 2021CFB115 and No 2021CFB608).

Competing interests No, there are no competing interests.

Patient consent for publication Not applicable.

Ethics approval The Ethics Committee of Wuhan Union Hospital (UHCT-IEC-SOP-016-03-01) approved all aspects of the study with informed consent from all patients. Tongji Medical College's Institutional Animal Care and Research Advisory Committee (IACUC number: 3402) approved all animal experiments conducted in the laboratory, per the NIH Guidelines for the Care and Use of Laboratory Animals. Participants gave informed consent to participate in the study before taking part.

Provenance and peer review Not commissioned; externally peer reviewed.

Data availability statement All data relevant to the study are included in the article or uploaded as supplementary information.

Supplemental material This content has been supplied by the author(s). It has not been vetted by BMJ Publishing Group Limited (BMJ) and may not have been peer-reviewed. Any opinions or recommendations discussed are solely those of the author(s) and are not endorsed by BMJ. BMJ disclaims all liability and responsibility arising from any reliance placed on the content. Where the content includes any translated material, BMJ does not warrant the accuracy and reliability of the translations (including but not limited to local regulations, clinical guidelines, terminology, drug names and drug dosages), and is not responsible for any error and/or omissions arising from translation and adaptation or otherwise.

Open access This is an open access article distributed in accordance with the Creative Commons Attribution Non Commercial (CC BY-NC 4.0) license, which permits others to distribute, remix, adapt, build upon this work non-commercially, and license their derivative works on different terms, provided the original work is properly cited, appropriate credit is given, any changes made indicated, and the use is non-commercial. See <http://creativecommons.org/licenses/by-nc/4.0/>.

ORCID iD

Rong Fu <http://orcid.org/0000-0002-7342-263X>

REFERENCES

- Lapointe S, Perry A, Butowski NA. Primary brain tumours in adults. *Lancet* 2018;392:432–46.
- Tan AC, Ashley DM, López GY, et al. Management of glioblastoma: state of the art and future directions. *CA Cancer J Clin* 2020;70:299–312.
- Ostrom QT, Bauchet L, Davis FG, et al. The epidemiology of glioma in adults: a "state of the science" review. *Neuro Oncol* 2014;16:896–913.
- Reck M, Rodríguez-Abreu D, Robinson AG, et al. Pembrolizumab versus chemotherapy for PD-L1-positive non-small-cell lung cancer. *N Engl J Med* 2016;375:1823–33.
- Sharma P, Allison JP. The future of immune Checkpoint therapy. *Science* 2015;348:56–61.
- Herbst RS, Soria J-C, Kowanetz M, et al. Predictive correlates of response to the anti-PD-L1 antibody Mpd3280A in cancer patients. *Nature* 2014;515:563–7.
- Iwai Y, Ishida M, Tanaka Y, et al. Involvement of PD-L1 on tumor cells in the escape from host immune system and tumor Immunotherapy by PD-L1 blockade. *Proc Natl Acad Sci U S A* 2002;99:12293–7.
- Garber ST, Hashimoto Y, Weathers S-P, et al. Immune Checkpoint blockade as a potential therapeutic target: surveying CNS malignancies. *Neuro Oncol* 2016;18:1357–66.
- Berghoff AS, Kiesel B, Widhalm G, et al. Programmed death ligand 1 expression and tumor-infiltrating lymphocytes in glioblastoma. *Neuro Oncol* 2015;17:1064–75.
- Quiros PM, Langer T, López-Otín C. New roles for mitochondrial proteases in health, ageing and disease. *Nat Rev Mol Cell Biol* 2015;16:345–59.
- Guo X, Aviles G, Liu Y, et al. Mitochondrial stress is relayed to the Cytosol by an Oma1-Dele1-HRI pathway. *Nature* 2020;579:427–32.
- Wu Z, Zuo M, Zeng L, et al. Oma1 Reprograms metabolism under hypoxia to promote colorectal cancer development. *EMBO Rep* 2021;22:e50827.
- Ahola S, Rivera Mejías P, Hermans S, et al. Oma1-mediated integrated stress response protects against Ferroptosis in mitochondrial cardiomyopathy. *Cell Metab* 2022;34:1875–91.
- Li J, Liao T, Liu H, et al. Hypoxic glioma stem cell-derived Exosomes containing Linc01060 promote progression of glioma by regulating the Mzf1/C-Myc/Hif1Alpha axis. *Cancer Res* 2021;81:114–28.
- Li J, Wang K, Yang C, et al. Tumor-associated macrophage-derived Exosomal Linc01232 induces the immune escape in glioma by decreasing surface MHC-I expression. *Advanced Science* 2023;10:e2207067.
- Li J, Yuan H, Xu H, et al. Hypoxic cancer-secreted Exosomal miR-182-5p promotes glioblastoma angiogenesis by targeting Kruppel-like factor 2 and 4. *Molecular Cancer Research* 2020;18:1218–31.
- Tang N, Zhu K, Jiang C, et al. Rnf7 promotes glioma growth via the Pi3K/AKT signalling axis. *J Cell Mol Med* 2023;27:277–86.
- Lonsdale J, Thomas J, Salvatore M, et al. Consortium GT: the genotype-tissue expression (Gtex) project. *Nat Genet* 2013;45:580–5.
- Li J, Shen J, Wang Z, et al. E1td1 facilitates glioma proliferation, migration and invasion by activating JAK/Stat3/HIF-1Alpha signaling axis. *Sci Rep* 2019;9:13904.
- Wang Z, Li J, Long X, et al. Mrps16 facilitates tumor progression via the Pi3K/AKT/snail signaling axis. *J Cancer* 2020;11:2032–43.
- Zong W-X, Rabinowitz JD, White E. Mitochondria and cancer. *Molecular Cell* 2016;61:667–76.
- Youle RJ, Narendra DP: mechanisms of Mitophagy. *Nat Rev Mol Cell Biol* 2011;12:9–14.
- Zhu J, Wang KZQ, Chu CT. Chu CT: after the banquet: mitochondrial Biogenesis, Mitophagy, and cell survival. *Autophagy* 2013;9:1663–76.
- Levy JMM, Towers CG, Thorburn A. Targeting Autophagy in cancer. *Nat Rev Cancer* 2017;17:528–42.
- Panigrahi DP, Prahara PP, Bhol CS, et al. The emerging, Multifaceted role of Mitophagy in cancer and cancer Therapeutics. *Seminars in Cancer Biology* 2020;66:45–58.
- Guo F, Liu X, Cai H, et al. Autophagy in neurodegenerative diseases: pathogenesis and therapy. *Brain Pathol* 2018;28:3–13.
- Liu J, Liu W, Li R, et al. Mitophagy in Parkinson's disease: from pathogenesis to treatment. *Cells* 2019;8:712:8.
- Ren J, Zhang Y. Targeting Autophagy in aging and aging-related cardiovascular diseases. *Trends Pharmacol Sci* 2018;39:1064–76.
- Bravo-San Pedro JM, Kroemer G, Galluzzi L. Autophagy and Mitophagy in cardiovascular disease. *Circ Res* 2017;120:1812–24.
- Vara-Perez M, Felipe-Abrio B, Agostinis P. Agostinis P: Mitophagy in cancer: A tale of adaptation. *Cells* 2019;8:493:8.
- Lu Y, Wang L, He M, et al. Nix protein positively regulates NF-kappaB activation in gliomas. *PLoS ONE* 2012;7:e44559.
- Favaro G, Romanello V, Varanita T, et al. Drp1-mediated mitochondrial shape controls calcium homeostasis and muscle mass. *Nat Commun* 2019;10:2576.
- Onishi M, Yamano K, Sato M, et al. Molecular mechanisms and physiological functions of Mitophagy. *EMBO J* 2021;40:e104705.
- Ashrafi G, Schwarz TL. The pathways of Mitophagy for quality control and clearance of mitochondria. *Cell Death Differ* 2013;20:31–42.
- Li J, Qi F, Su H, et al. Hspa9-Facilitated mitochondria-associated ER membrane (MAM) integrity controls cisplatin-resistance in ovarian cancer patients. *Int J Biol Sci* 2022;18:2914–31.
- Carneiro BA, El-Deiry WS. El-Deiry WS: targeting apoptosis in cancer therapy. *Nat Rev Clin Oncol* 2020;17:395–417.
- Zhong W, Rao Z, Xu J, et al. Defective Mitophagy in aged Macrophages promotes mitochondrial DNA cytosolic leakage to activate STING signaling during liver sterile inflammation. *Aging Cell* 2022;21:e13622.
- Liu Z, Wang M, Wang X, et al. Xbp1 deficiency promotes hepatocyte Pyroptosis by impairing Mitophagy to activate mtDNA-cGAS-STING signaling in Macrophages during acute liver injury. *Redox Biol* 2022;52:102305.
- Cheng AN, Cheng L-C, Kuo C-L, et al. Mitochondrial Lon-induced mtDNA leakage contributes to PD-L1-mediated Immunoescape via STING-IFN signaling and extracellular Vesicles. *J Immunother Cancer* 2020;8:e001372:8.
- Wang Y-A, Li X-L, Mo Y-Z, et al. Effects of tumor metabolic Microenvironment on regulatory T cells. *Mol Cancer* 2018;17:168.
- Yu J, Du W, Yan F, et al. Myeloid-derived Suppressor cells suppress antitumor immune responses through IDO expression and correlate with lymph node metastasis in patients with breast cancer. *J Immunol* 2013;190:3783–97.
- Benencia F, Muccioli M, Alnaeeli M. Perspectives on Reprogramming cancer-associated Dendritic cells for anti-tumor therapies. *Front Oncol* 2014;4:72.
- Jiang X, Wang J, Deng X, et al. Role of the tumor Microenvironment in PD-L1/PD-1-mediated tumor immune escape. *Mol Cancer* 2019;18:10.
- Brahmer JR, Tykodi SS, Chow LQM, et al. Safety and activity of anti-PD-L1 antibody in patients with advanced cancer. *N Engl J Med* 2012;366:2455–65.
- Sharma P, Callahan MK, Bono P, et al. Nivolumab monotherapy in recurrent metastatic urothelial carcinoma (Checkmate 032): a Multicentre, open-label, two-stage, multi-arm, phase 1/2 trial. *Lancet Oncol* 2016;17:1590–8.
- Motzer RJ, Escudier B, McDermott DF, et al. Nivolumab versus everolimus in advanced renal-cell carcinoma. *N Engl J Med* 2015;373:1803–13.
- Kobold S, Pantelyushin S, Rataj F, et al. Rationale for combining Bispecific T cell activating antibodies with Checkpoint blockade for cancer therapy. *Front Oncol* 2018;8:285.
- Popovic A, Jaffee EM, Zaidi N. Emerging strategies for combination Checkpoint Modulators in cancer Immunotherapy. *J Clin Invest* 2018;128:120775:3209–18.
- Li S, Yang F, Ren X. Immunotherapy for hepatocellular carcinoma. *Drug Discov Ther* 2015;9:363–71.

- 50 Carter BW, Halpenny DF, Ginsberg MS, *et al.* Immunotherapy in non-small cell lung cancer treatment: Current status and the role of imaging. *J Thorac Imaging* 2017;32:300–12.
- 51 Freeman GJ, Long AJ, Iwai Y, *et al.* Engagement of the PD-1 Immunoinhibitory receptor by a novel B7 family member leads to negative regulation of lymphocyte activation. *J Exp Med* 2000;192:1027–34.
- 52 Dong H, Strome SE, Salomao DR, *et al.* Tumor-associated B7-H1 promotes T-cell apoptosis: a potential mechanism of immune evasion. *Nat Med* 2002;8:793–800.
- 53 Schadendorf D, Hodi FS, Robert C, *et al.* Pooled analysis of long-term survival data from phase II and phase III trials of Ipilimumab in Unresectable or metastatic Melanoma. *J Clin Oncol* 2015;33:1889–94.
- 54 Topalian SL, Hodi FS, Brahmer JR, *et al.* Safety, activity, and immune correlates of anti-PD-1 antibody in cancer. *N Engl J Med* 2012;366:2443–54.
- 55 Brahmer J, Reckamp KL, Baas P, *et al.* Nivolumab versus Docetaxel in advanced squamous-cell non–small-cell lung cancer. *N Engl J Med* 2015;373:123–35.
- 56 Muenst S, Soysal SD, Gao F, *et al.* The presence of programmed death 1 (PD-1)-Positive tumor-infiltrating lymphocytes is associated with poor prognosis in human breast cancer. *Breast Cancer Res Treat* 2013;139:667–76.
- 57 Chapon M, Randriamampita C, Maubec E, *et al.* Progressive upregulation of PD-1 in primary and metastatic Melanomas associated with blunted TCR signaling in infiltrating T lymphocytes. *J Invest Dermatol* 2011;131:1300–7.
- 58 Boutros C, Tarhini A, Routier E, *et al.* Safety profiles of anti-CTLA-4 and anti-PD-1 antibodies alone and in combination. *Nat Rev Clin Oncol* 2016;13:473–86.
- 59 Muenst S, Schaerli AR, Gao F, *et al.* Expression of programmed death ligand 1 (PD-L1) is associated with poor prognosis in human breast cancer. *Breast Cancer Res Treat* 2014;146:15–24.
- 60 Chinai JM, Janakiram M, Chen F, *et al.* New Immunotherapies targeting the PD-1 pathway. *Trends Pharmacol Sci* 2015;36:587–95.
- 61 Chen G, Huang AC, Zhang W, *et al.* Exosomal PD-L1 contributes to immunosuppression and is associated with anti-PD-1 response. *Nature* 2018;560:382–6.
- 62 Tilokani L, Nagashima S, Paupe V, *et al.* Mitochondrial Dynamics: overview of molecular mechanisms. *Essays Biochem* 2018;62:341–60.
- 63 Wai T, Langer T. Mitochondrial Dynamics and metabolic regulation. *Trends Endocrinol Metab* 2016;27:105–17.
- 64 Vásquez-Trincado C, García-Carvajal I, Pennanen C, *et al.* Mitochondrial Dynamics, Mitophagy and cardiovascular disease. *J Physiol* 2016;594:509–25.
- 65 Abeliovich H, Zarei M, Rigbolt KTG, *et al.* Involvement of mitochondrial Dynamics in the segregation of mitochondrial matrix proteins during stationary phase Mitophagy. *Nat Commun* 2013;4:2789.
- 66 Hasanovic A, Mus-Veteau I. Mus-Veteau I: targeting the multidrug transporter Ptcp1 potentiates chemotherapy efficiency. *Cells* 2018;7:107:7:.
- 67 Wang Y, Liu HH, Cao YT, *et al.* The role of mitochondrial Dynamics and Mitophagy in carcinogenesis, metastasis and therapy. *Front Cell Dev Biol* 2020;8:413.
- 68 Pérez-Ruiz E, Melero I, Kopecka J, *et al.* Cancer Immunotherapy resistance based on immune checkpoints inhibitors: targets, biomarkers, and remedies. *Drug Resist Updat* 2020;53:100718.